Asteroids, Comets, Meteors
Proceedings IAU Symposium No. 229, 2005
D. Lazzaro, S. Ferraz-Mello & J.A. Fernández, eds.

doi:10.1017/S1743921305006800

Asteroid families

David Nesvorný[1], William F. Bottke[1], David Vokrouhlický[2], Alessandro Morbidelli[3] and Robert Jedicke[4]

[1]Department of Space Studies, Southwest Research Institute, 1050 Walnut St., Suite 400, Boulder, CO 80302, USA, email: davidn@boulder.swri.edu

[2]Institute of Astronomy, Charles University, V Holešovickách 2, CZ-18000 Prague 8, Czech Republic

[3]Observatoire de la Côte D'Azur, Dept. Cassiopee, BP 4224, 06304 Nice Cedex 4, France

[4]Institute for Astronomy, University of Hawaii, 2680 Woodlawn Drive, Honolulu, HI 96822, USA

Abstract. An asteroid family is a group of asteroids with similar orbits and spectra that was produced by a collisional breakup of a large parent body. To identify asteroid families, researchers look for clusters of asteroid positions in the space of proper orbital elements. These elements, being more constant over time than osculating orbital elements, provide a dynamical criterion of whether a group of bodies has a common ancestor. More than fifty asteroid families have been identified to date. Their analysis produced several important insights into the physics of large scale collisions, dynamical processes affecting small bodies in the Solar System, and surface and interior properties of asteroids.

Keywords. minor planets, asteroids

1. Introduction

The asteroid belt has collisionally evolved since its formation (see Davis *et al.* 2002 and other chapters in section 4.2 of the *Asteroids III* book). Possibly its most striking feature is the asteroid families that represent remnants of large, collisionally disrupted asteroids (Hirayama 1918; Zappalà *et al.* 1995). In the present asteroid belt most asteroid families can be clearly distinguished from the background population of asteroids.

To analyze these sets separately, we will sort the main-belt asteroids into family and background populations. The analysis of the asteroid families may tell us about things such as asteroid interiors, geological differentiation in the main belt, or about phenomena that alter asteroid colors with time. The analysis of background asteroids is more related to issues such as the primordial temperature gradient in the proto-planetary nebula, subsequent dynamical excitation and mixing of bodies formed at different orbital distances from the Sun.

Here we review the problem of identification of asteroid families in large catalogs of proper elements (section 2). Table 1 lists all asteroid families identified here along with information about the number of family members, size of the parent body, family's age and spectroscopic properties. Sections 3–6 briefly review the methods used to determine these properties and lists relevant references. All families described here are in the main belt and have inclinations $i < 17$ deg; high-inclination main-belt families and families in Jupiter's Trojan swarms are not discussed.

2. Identification

To identify asteroid families, researchers look for clusters of asteroid positions in the space of proper elements: the proper semimajor axis ($a_{\rm P}$), proper eccentricity ($e_{\rm P}$), and proper inclination ($i_{\rm P}$) (Milani & Knežević 1994; Knežević *et al.* 2002). These orbital elements describe the size, shape and tilt of orbits. Proper orbital elements, being more constant over time than instantaneous orbital elements, provide a dynamical criterion of whether or not a group of bodies has a common ancestor.

We used a numerical code that automatically detects a cluster of asteroid positions in the 3-dimensional space of proper elements. We based our code on the Hierarchical Clustering Method (hereafter HCM, Zappalà *et al.* 1990). The HCM requires that members of the identified cluster of asteroid positions in the proper elements space be separated by less than a selected distance (the so-called 'cutoff').

In the first step, we applied the HCM to a catalog of proper asteroid elements (Milani & Knežević 1994; Knežević *et al.* 2002). The catalog we used for this work is already dated. It included 106,284 proper elements known back in 2003. The most recent release of the proper element catalog includes almost 170,000 entries.

The HCM starts with an individual asteroid position in the space of proper elements and identifies bodies in its neighborhood with mutual distances less than a threshold limit ($d_{\rm cutoff}$). We defined the distance in $(a_{\rm P}, e_{\rm P}, i_{\rm P})$ space by

$$d = na_{\rm P}\sqrt{C_a(\delta a_{\rm P}/a_{\rm P})^2 + C_e(\delta e_{\rm P})^2 + C_i(\delta \sin i_{\rm P})^2}, \tag{2.1}$$

where $na_{\rm P}$ is the heliocentric velocity of an asteroid on a circular orbit having the semimajor axis $a_{\rm P}$. $\delta a_{\rm P} = |a_{\rm P}^{(1)} - a_{\rm P}^{(2)}|$, $\delta e_{\rm P} = |e_{\rm P}^{(1)} - e_{\rm P}^{(2)}|$, and $\delta \sin i_{\rm P} = |\sin i_{\rm P}^{(1)} - \sin i_{\rm P}^{(2)}|$. The indexes (1) and (2) denote the two bodies in consideration. C_a, C_e and C_i are weighting factors; we adopted $C_a = 5/4$, $C_e = 2$ and $C_i = 2$ (Zappalà *et al.* 1994). Other choices of C_a, C_e and C_i yield similar results.

The cutoff distance $d_{\rm cutoff}$ is a free parameter. With small $d_{\rm cutoff}$ the algorithm identifies tight clusters in the proper element space. With large $d_{\rm cutoff}$ the algorithm detects larger and more loosely connected clusters. For the main belt, the appropriate values of $d_{\rm cutoff}$ are between 1 and 150 m/s. To avoid an a priori choice of $d_{\rm cutoff}$, we developed software that runs HCM starting with each individual asteroid in our sample and loops over 150 values of $d_{\rm cutoff}$ between 1 and 150 m/s with a 1 m/s step.

In Fig. 1, we illustrate the final product of this algorithm using a 'stalactite' diagram (Zappalà *et al.* 1990, 1994). For each $d_{\rm cutoff}$ on the Y-axis we plot all clusters found by the HCM. For example, with $d_{\rm cutoff} = 150$ m/s, nearly the whole main belt is linked to a single asteroid, (1) Ceres. We plot a horizontal line segment at $d_{\rm cutoff} = 150$ m/s with length equal to the total number of members in this cluster. At smaller $d_{\rm cutoff}$ the complex structure of the main asteroid belt emerges. The stalactite diagram is extremely useful when we want to systematically classify this information. In fact, more than fifty significant groups are shown in Fig. 1 – twice the number of robust asteroid families known previously (Bendjoya & Zappalà 2002). We label each stalactite by the lowest numbered asteroid in the group (not all these labels appear in Fig. 1), and proceed to the second step of our algorithm.

In the second step, we select appropriate $d_{\rm cutoff}$ for each individual cluster. Unlike the first step of our algorithm that is fully automated, the second step requires some non-trivial insight into the dynamics of the main-belt asteroids, and cannot be fully automated. To correlate values of $d_{\rm cutoff}$ with structures and processes operating in the main belt, we analyzed projections of families into $(a_{\rm P}, e_{\rm P})$ and $(a_{\rm P}, i_{\rm P})$ planes. Moreover, we used an interactive visualization tool that allows us to work in three dimensions thus

https://doi.org/10.1017/S1743921305006800 Published online by Cambridge University Press

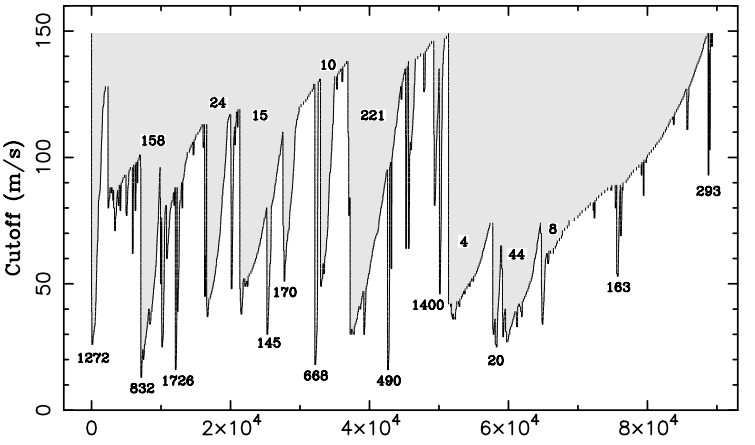

Figure 1. The dynamical structure of the asteroid belt represented in the 'stalactite diagram'. Each stalactite represents an asteroid family and is labeled by the member asteroid that has the lowest designation number. The width of a stalactite at cutoff d shows the number of family members that were identified with d. Large families, such as those associated with (158) Koronis, (24) Themis, (15) Eunomia, (221) Eos, (4) Vesta, and (44) Nysa, appear as thick stalactites that persist over a large range of $d_{\rm cutoff}$. Smaller families are represented by thin stalactites that are often (but not always, see, e.g., no. 490 corresponding to the Veritas family) vertically short meaning that their determination requires a specific narrow range of $d_{\rm cutoff}$.

avoiding problems generated by the projection effects into either $(a_{\rm P}, e_{\rm P})$ or $(a_{\rm P}, i_{\rm P})$ planes.

The final product of our algorithm are the asteroid families (Table 1), lists of their members selected at appropriate cutoffs, and the list of background asteroids showing no apparent groups. Figure 2 illustrates this result. From the total of 106,284 main-belt asteroids used here, 38,625 are family members (36.3% of total) and 67,659 are background asteroids (63.7%).

To determine whether our algorithm produced a reasonably complete list of asteroid families, we searched for residual clusters in the background asteroid population using proper elements and asteroid colors simultaneously. Asteroid colors were taken from the Sloan Digital Sky Survey Moving Object Catalog (Ivezić *et al.* 2001; Stoughton *et al.* 2002). We defined the distance in $(a_{\rm P}, e_{\rm P}, i_{\rm P}, {\rm PC}_1, {\rm PC}_2)$ space (see section 5 for the definition of principal color components $\rm PC_1$ and $\rm PC_2$) by

$$d_2 = \sqrt{d^2 + C_{\rm PC}[(\delta {\rm PC}_1)^2 + (\delta {\rm PC}_2)^2]}, \tag{2.2}$$

where d is the distance in $(a_{\rm P}, e_{\rm P}, i_{\rm P})$ sub-space defined in Eq. (2.1), $\delta {\rm PC}_1 = |{\rm PC}_1^{(1)} - {\rm PC}_1^{(2)}|$, and $\delta {\rm PC}_2 = |{\rm PC}_2^{(1)} - {\rm PC}_2^{(2)}|$. The indexes (1) and (2) denote the two bodies in consideration. $C_{\rm PC}$ is a factor that weights the relative importance of colors in our generalized HCM search. With d in ${\rm m\,s^{-1}}$, we used typically $C_{\rm PC} = 10^6$ and varied this factor in the 10^4–10^8 range to test the dependence of results. For $C_{\rm PC} < 10^4$ the principal components are given too little weight to be useful. For $C_{\rm PC} > 10^8$ the orbital information, which is essential for correct family identification, is not appropriately used.

We have found no statistically robust concentrations in the extended proper element/color space that would help us to identify new families. This result shows that the list of families in Table 1 based on the available data is (at least nearly) complete. We have also found that the generalized HCM search is useful to identify family 'halos', i.e., populations of peripheric family members that were not joined with the rest of the

https://doi.org/10.1017/S1743921305006800 Published online by Cambridge University Press

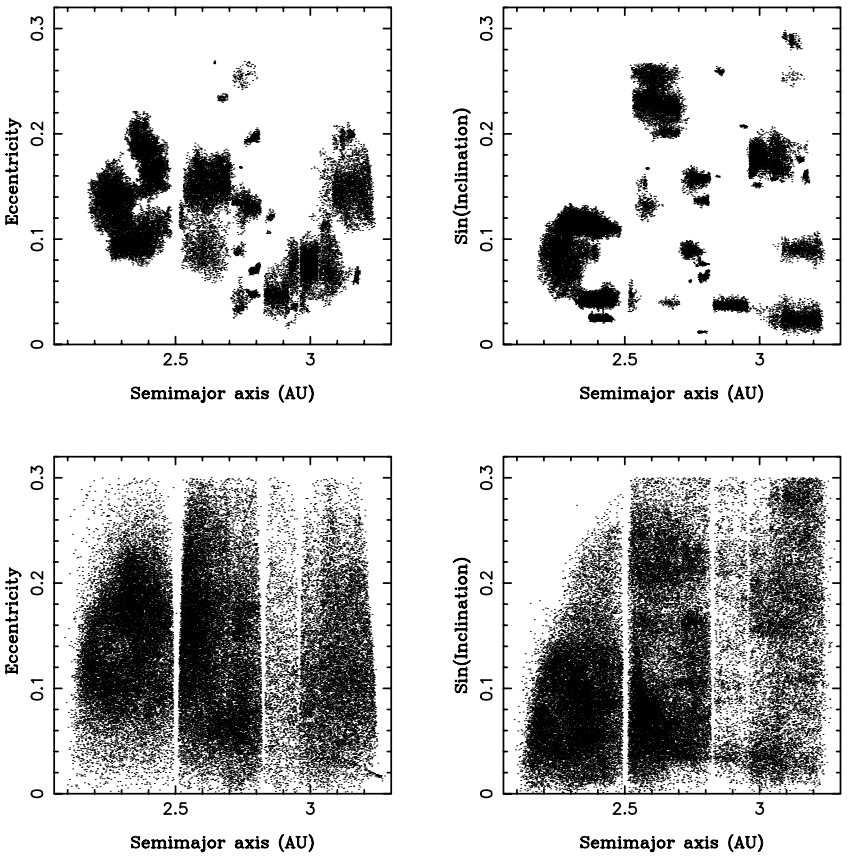

Figure 2. Decomposition of the asteroid belt into family and background asteroids. From top to bottom, the panels show the orbit distribution of the family members and background asteroids, respectively.

family with the standard HCM and cutoffs listed in Table 1. For example, the Koronis family halo located at $a_{\rm P} = 2.9$ AU and small $i_{\rm P}$ can be clearly identified. Other 'halos', such as ∼30 additional peripheric members of the Nysa-Polana (Cellino *et al.* 2001) family can be identified only in the extended proper element/color space, because their color differs from thet of the local background ($\rm PC_1 \lesssim 0$ for the Polana family).

By choosing cutoff distances d, we compromised (i) to include as many peripheric family members as possible, and (ii) to avoid including too many peripheric interlopers. The selected values of d that are listed in Table 1 are usually restrictive (i.e., at the small end of the acceptable range) because one of the goals of our study is to determine the reliable mean colors for family members. We thus tried to avoid including many peripheric interlopers by using small d.

In total, we have identified ∼50 statistically robust asteroid families. We list 42 selected main-belt families in Table 1 (i.e., the Pallas family, high-i or non-main-belt families, and several sub-structures of the prominent main-belt families are not listed). Table 1 includes all most-reliable asteroid families listed in Bendjoya & Zappalà (2002; 25 in total) except a dispersed clump of asteroids around (110) Lydia (Zappalà *et al.* 1994, 1995) which the HCM failed to identify in the new catalog of proper elements. The large overlap between our and previous family classifications shows the consistency of our approach.

https://doi.org/10.1017/S1743921305006800 Published online by Cambridge University Press

By using more proper elements than previous studies we found ≈20 new, statistically-robust asteroid families.

3. Size-Frequency Distribution

The Size-Frequency Distribution (hereafter SFD) of observed families is much steeper than that of the local background for absolute magnitudes $H < 13$ (see Zappalà *et al.* 2002 for a review, and Morbidelli *et al.* 2003 for a definition of the local background). If this steep SFD is extrapolated to $H > 13$, small asteroid family members would become more numerous than small background asteroids. That is not what actually happens. Morbidelli *et al.* (2003) have shown that the debiased SFD of asteroid families is shallower than that of the background for $H > 15$ and that the number of family members does not exceed the number of background asteroids down to $H \approx 18$. In fact, the asteroid families probably represent about 30-40% of the main belt population of asteroids down to $D = 1$ km.

4. Size of the parent body

Durda *et al.* (2005) used hydrodynamic modeling of impacts to determine the diameter of the parent body, $D_{\rm PB}$, for 28 families. In essence, they searched for a combination of impact paremeters (including $D_{\rm PB}$) that produced best fits to the observed SFD of large family members (assuming this distribution did not change by secondary fragmentations; Bottke *et al.* 2005). The same method has been recently applied to the Karin cluster yielding $D_{\rm PB} = 31 \pm 3$ km (Nesvorný *et al.* 2005a). The hydrodynamic method avoids problems with the observational incompletness at small sizes and is more rooted in impact physics that the geometrical approch used by Tanga *et al.* (1999).

Table 1 lists $D_{\rm PB}$, $D_{\rm LF}$ and $M_{\rm LF}/M_{\rm PB}$, where $D_{\rm LF}$ is the effective diameter of the largest fragment and $M_{\rm LF}/M_{\rm PB}$ is the largest fragment to parent body mass ratio. $D_{\rm PB}$ that appear in parenthesis in Table 1 were estimated from the observed, observationally-incomplete population of family members. In these cases, true $D_{\rm PB}$ is likely to be larger than the values listed in Table 1. $D_{\rm LF}$ was taken from the SIMPS database (Tedesco *et al.* 2002) or was estimated from the absolute magnitude of the object and albedo appropriate for its taxonomic class. Values estimated via latter method appear in parenthesis in Table 1. Diameter values and $M_{\rm LF}/M_{\rm PB}$ for Bower and Brasilia families are uncertain because 1639 Bower and 293 Brasilia may be interlopers within their own families.

Tanga *et al.* (1999) determined $D_{\rm PB}$ for 14 families using pre-1999 catalog of proper elements and a geometrical approach (see Tanga *et al.* 1999 for a detail description of their method). In general, values listed in Table 1 are similar to those of Tanga *et al.* In many cases, however, the hydrodynamic method combined with our more complete sample of family members produces substantially larger $D_{\rm PB}$. A major disagreement occurs for Eos, Dora, Gefion and Merxia families where hydrodynamic $D_{\rm PB}$ are much larger than Tanga *et al.* ' $D_{\rm PB}$. For Dora and Gefion families, the discrepancy may be (at least partially) understood because Durda *et al.* did not obtain good fits for these families via hydrodynamic modeling. Conversely, Eos and Merxia families for which Durda *et al.* 's fits were good may have larger $D_{\rm PB}$ than thought before.

In total, Table 1 lists estimates of $D_{\rm PB}$ for 35 asteroid families. Out of these, 27 families have $D_{\rm PB} > 100$ km, 24 families correspond to catastrophic breakups ($M_{\rm LF}/M_{\rm PB} \leqslant 0.5$), 4 families were produced by cratering impacts (Juno, Vesta, Massalia, Nemesis; $M_{\rm LF}/M_{\rm PB} \geqslant 0.9$), 10 families correspond to super-catastrophic breakups ($M_{\rm LF}/M_{\rm PB} \leqslant 0.1$), and 19 families have $D_{\rm PB} > 100$ km and $M_{\rm LF}/M_{\rm PB} \leqslant 0.5$. Note that these numbers

https://doi.org/10.1017/S1743921305006800 Published online by Cambridge University Press

Table 1. List of identified, statistically-robust asteroid families. The columns are: lowest-numbered asteroid family member; cutoff limit used ($d_{\rm cutoff}$); number of family members determined with $d_{\rm cutoff}$; common taxonomic type(s) of family members; mean PC_1 and PC_2 values from SDSS; age of the family, when available; diameter of the parent body ($D_{\rm PB}$); diameter of the largest fragment ($D_{\rm LF}$); and largest fragment to parent body mass ratio ($M_{\rm LF}/M_{\rm PB}$). Meaning of parenthesis for $D_{\rm PB}$ and $D_{\rm LF}$ values is explained in section 3.2.

Family	$d_{\rm cutoff}$ (m/s)	# of mem.	Tax. Type	PC_1	PC_2	Age (My)	$D_{\rm PB}$ (km)	$D_{\rm LF}$ (km)	$M_{\rm LF}/M_{\rm PB}$ Mass Ratio
Inner Main Belt, $2.0 < a < 2.5$ *AU*									
4 Vesta	70	5575	V	0.491	-0.288	–	(471)	468	0.98
8 Flora	80	6131	S	–	–	1000 ± 500	203	136	0.3
20 Massalia	50	966	S	0.493	-0.139	150 ± 20	146	146	$\approx$1
44 Nysa(Polana)	60	4744	S(F)	–	–	–	–	–	–
163 Erigone	80	410	C/X	0.138	-0.131	280 ± 50	114	73	0.26
Central Main Belt, $2.5 < a < 2.82$ *AU*									
3 Juno	50	74	S	0.523	-0.150	–	(234)	234	$\approx$1
15 Eunomia	80	3830	S	0.624	-0.156	2500 ± 500	$\approx$300	255	$\approx$0.6
46 Hestia	80	154	S	0.624	-0.151	–	156	124	0.50
128 Nemesis	70	133	C	0.189	-0.196	200 ± 100	195	188	0.90
145 Adeona	60	533	Ch	0.112	-0.189	700 ± 500	184	151	0.55
170 Maria	100	1621	S/L	0.578	-0.107	3000 ± 1000	192	44	0.01
363 Padua	70	303	X/C	0.273	-0.122	300 ± 200	106	(75)	$\approx$0.35
396 Aeolia	20	28	–	0.270	-0.187	–	39	34	0.66
410 Chloris	120	135	C	0.241	-0.093	700 ± 400	$\approx$175	124	$\approx$ 0.35
569 Misa	80	119	C	0.154	-0.185	500 ± 200	117	73	0.24
606 Brangane	30	30	S	0.441	0.061	50 ± 40	46	36	0.48
668 Dora	70	404	Ch	0.091	-0.190	500 ± 200	$\approx$165	27	$\approx$0.004
808 Merxia	100	271	S/Sq	0.455	-0.115	240 ± 50	121	33	0.02
847 Agnia	40	252	S/Sq	0.435	-0.169	100 ± 30	60	28	0.10
1128 Astrid	50	65	C	0.221	-0.210	180 ± 80	(41)	35	$\approx$0.6
1272 Gefion	80	973	S	0.544	-0.123	1200 ± 400	212	(35)	$\approx$0.005
1639 Bower	100	82	–	0.528	0.026	–	(52)	36	$\approx$0.3
1644 Rafita	100	382	S	0.538	-0.127	1500 ± 500	63	(42)	$\approx$0.3
1726 Hoffmeister	50	235	C	0.058	-0.115	300 ± 200	134	26	0.007
2980 Cameron	60	162	S	0.518	-0.116	–	–	–	–
4652 Iannini	30	18	S	0.324	-0.109	$\lesssim$5	–	–	–
Outer Main Belt, $2.82 < a < 3.5$ *AU*									
10 Hygiea	80	1136	C/B	0.081	-0.170	2000 ± 1000	443	407	0.78
24 Themis	90	2398	C/B	0.092	-0.179	2500 ± 1000	448	(225)	$\approx$0.13
87 Sylvia	60	19	–	0.137	0.033	–	272	260	0.87
137 Meliboea	120	57	Ch	0.185	-0.161	–	242	145	0.22
158 Koronis	70	2304	S	0.522	-0.111	2500 ± 1000	166	35	0.01
221 Eos	80	4412	K/T/D	0.466	-0.104	1300 ± 200	401	104	0.02
283 Emma	40	76	–	0.129	-0.053	–	185	148	0.51
293 Brasilia	80	95	C/X	0.222	-0.076	50 ± 40	206	55	0.02
490 Veritas	50	284	Ch	0.212	-0.230	8.3 ± 0.5	177	115	0.27
832 Karin	10	84	S	0.387	-0.228	5.8 ± 0.2	31 ± 3	(17)	$\approx$ 0.16
845 Naema	40	64	C	0.135	-0.178	100 ± 50	81	54	0.30
1400 Tirela	70	212	D	0.714	-0.128	–	–	–	–
3556 Lixiaohua	50	97	C/X	0.170	-0.080	300 ± 200	203	30	0.003
9506 Telramund	60	70	S	0.502	-0.166	–	–	–	–
18405 FY12	50	11	X	0.214	0.001	–	–	–	–

https://doi.org/10.1017/S1743921305006800 Published online by Cambridge University Press

do not include Nysa/Polana complex which we did not resolve into two families via HCM. These numbers provide important constraints on the collisional history of the main belt.

5. Spectral properties

Taxonomic classification of asteroid families from visible spectroscopy was recently reviewed by Cellino *et al.* (2002) and Mothé-Diniz *et al.* (2005) (see also Bus & Binzel 2002a, 2002b). The principal result of spectroscopic studies is that members of an asteroid family show similar reflectance spectra. This has been taken as an evidence that main belt asteroids generally have non-differentiated interiors. Nevertheless, important variation of spectral properties can exist among different members of a single dynamical family probably due to somewhat heterogenous composition of the parent asteroid.

Spectroscopy is particularly useful to identify interlopers within families. These objects have the taxonomic type which is typical for background asteroids at the semimajor axis location of a family (S in the inner main belt, C in the outer main belt) and which contrasts with the family's own taxonomic class. For example, asteroids no. 100, 108, 1109, 1209 and 1599 are spectroscopic interlopers in the Hygiea family, asteroids no. 85 and 141 in the Eunomia family, asteroids no. 423 and 507 in the Eos family, asteroids no. 83, 255 and 481 in the Gefion family. It is important to exclude these large interlopers.

Our Table 1 includes 24 families that were not listed in Cellino *et al.* (2002) because their taxonomic type was not known previously. On the other hand, Cellino *et al.* listed 11 families that are not included in our Table 1. Four of these families (14 Bellona, 88 Thisbe, 226 Weringia, 729 Watsonia) are very dispersed asteroid groups in proper element space and have been identified by means of spectroscopy rather than by the analysis of the proper elements. The (2) Pallas family is not included in our list because (2) Pallas has highly inclined orbit and does not appear in the catalog of analytically calculated proper elements that we use here. Three of Cellino *et al.* 's families (125 Liberatrix, 237 Coelestina, 322 Phaeo) were identified by means of the wavelet analysis of the proper elements. These families are statistically less robust because the wavelet analysis is known to impose more relaxed criteria on family membership than the HCM (Zappalà *et al.* 1995). The (2085) Henan and (110) Lydia families are rather dispersed, possibly old families that we have failed to identify as reliable asteroid families by using the most recent proper element catalog. Finally, the HCM fails to identify Cellino *et al.* 's (45) Eugenia family with $d \leqslant 120$ m/s, while all our other families show many members with $d \leqslant 120$ m/s values.

Significant color variation exist between different asteroid families partly because of the varying mineralogy of their parent asteroids and probably also due effects of space weathering (Jedicke *et al.* 2004; Nesvorný *et al.* 2005b). Table 1 lists the color information for 40 asteroid families. Asteroid colors were taken from the Sloan Digital Sky Survey Moving Object Catalog, hereafter SDSS MOC. The second release of SDSS MOC includes five-color CCD photometry for 125,283 moving objects (Ivezić *et al.* 2001; Stoughton *et al.* 2002).

35,401 unique moving objects detected by the survey (i.e., about 28% of the total) have been matched (Jurić *et al.* 2002) to known asteroids listed in the ASTORB file (Bowell *et al.* 1994). The flux reflected by the detected objects was measured almost simultaneously in five bands (measurements in two successive bands were separated in time by 72 seconds) with effective wavelengths 3557 Å (u band), 4825 Å (g band), 6261 Å (r band), 7672 Å (i band), and 9097 Å (z band), and with 0.1-0.3μm band widths (Fukugita *et al.* 1996). The SDSS photometry is broadly consistent with published spectra of asteroids (Nesvorný *et al.* 2005b).

https://doi.org/10.1017/S1743921305006800 Published online by Cambridge University Press

To make an efficient use of the SDSS MOC, we utilized the Principal Component Analysis (hereafter PCA). The PCA involves a mathematical procedure that transforms a number of possibly correlated variables into a smaller number of uncorrelated variables called principal components. The first principal component accounts for as much of the variability in the data as possible, and each succeeding component accounts for as much of the remaining variability as possible. In the result, the PCA creates linear combinations of the five SDSS colors that maximize the separation between the taxonomic types in the SDSS data.

The first two principal components (i.e., the new uncorrelated variables) that this algorithm yields are given by the following relationships:

$$\begin{aligned} \mathrm{PC}_1 &= 0.396(u-g) + 0.553(g-r) + 0.567(g-i) + 0.465(g-z) \\ \mathrm{PC}_2 &= -0.819(u-g) + 0.017(g-r) + 0.09(g-i) + 0.567(g-z), \end{aligned} \tag{5.1}$$

where u, g, r, i, z are the measured fluxes in five bands after correction for solar colors.

We used the subset of entries in the SDSS MOC that were matched to asteroids with known orbit elements (Jurić *et al.* 2002) and that have $\delta\mathrm{PC}_1 < 0.1$ and $\delta\mathrm{PC}_2 < 0.1$, where $\delta\mathrm{PC}_1$ and $\delta\mathrm{PC}_2$ are the measurement errors in the principal components. In total, we studied colors of 7,593 main-belt asteroids of which 3,026 are family members and 4,567 are background main belt objects.

Table 1 lists mean values of PC_1 and PC_2 for individual families. In cases where the taxonomic type of a family was known previously from observations of its large members (see Cellino *et al.* 2002 and references therein) we found that the PC_1 value suggests that this type is also predominant for small asteroid family members observed by the SDSS (see also Ivezić *et al.* 2002).

Figure 3 shows the mean colors of S-, C- and X-complex families. The S-complex families have $\mathrm{PC}_1 > 0.35$ while C- and X-complex families have $\mathrm{PC}_1 < 0.35$. The V-type Vesta family (denoted in green) differs from the S-type families by small PC_2. The (832) Karin cluster and the (490) Veritas family, the two youngest known asteroid families for which we have good color data, are located on a periphery of regions in $(\mathrm{PC}_1, \mathrm{PC}_2)$ plane that are populated by the S- and C-type families. There is a significant spread of PC_1 and PC_2 for families of the same taxonomic complex. For example, two C-complex families can differ by $\sim$0.1-0.2 in PC_1 and/or PC_2. Because measurement errors and errors of the mean colors are $\lesssim$0.05, Fig. 3 documents true color differences between families. This result is consistent with studies of spectral variability among families by higher-resolution spectrophotometric measurements (Cellino *et al.* 2002).

6. Age

Accurate determination of the age of an asteroid family can obtained by modeling of orbital dynamics and dispersal of family members via effects of the Yarkovsky force (see Bottke *et al.* 2002 for a review of the Yarkovsky effect). Two different methods have been used to date:

1. Backward Numerical Integration of Orbits. To determine the exact age of a young family, the orbits of the family members can be numerically integrated into the past. The goal is to show that in some previous epoch the orbits of all cluster members were nearly the same (Nesvorný *et al.* 2002). There are two angles that determine the orientation of an orbit in space: the longitude of the ascending node (Ω) and the argument of perihelion (ω). Due to planetary perturbations these angles evolve with different but nearly constant speeds for individual asteroid orbits. Today, the orbits of the family members are oriented

https://doi.org/10.1017/S1743921305006800 Published online by Cambridge University Press

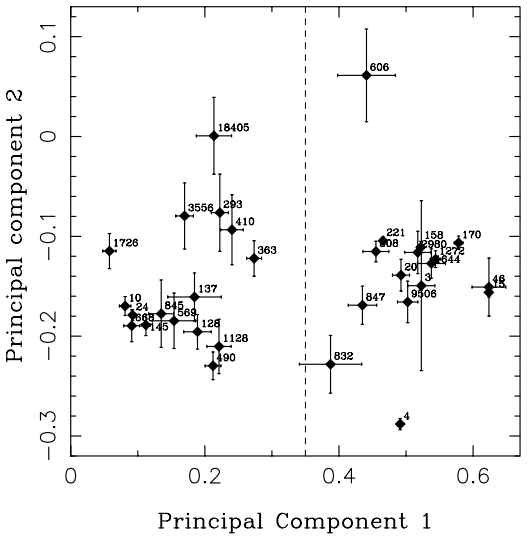

Figure 3. Principal color components PC_1 and PC_2 for asteroid families: PC_1 is a proxy for the spectral slope and PC_2 is related to the spectral curvature (Nesvorný *et al.* 2005b). The bars show 1-σ errors of mean PC_1 and PC_2. Only families with at least two members matching various criteria are shown (see Nesvorný *et al.* 2005b). The C- and S-complex families clearly segregate in PC_1 by the vertical dashed line at $PC_1 = 0.35$. The mean colors of recently-formed Veritas (no. 490) and Karin (no. 832) families are located on a periphery of well defined regions in (PC_1, PC_2) plane that are populated by the C- and S-complex families, respectively. Note the large color difference between the (832) Karin and (158) Koronis families. The Vesta family (no. 4) has the smallest mean PC_2 value among the identified families; the Brangane family (no. 606) has the largest mean PC_2 value.

differently in space because their slightly dissimilar periods of Ω and ω produce slow differential rotation of their orbits with respect to each other. Eventually, this effect allows Ω and ω to obtain nearly uniform distributions in $[0°, 360°]$. For a short time after the parent body breakup, however, the orientations of the fragments' orbits must have been nearly the same. Nesvorný *et al.* (2002, 2003) used this method to determine the ages of the Karin (5.8 ± 0.2 My) and Veritas (8.3 ± 0.5 My) families, and also found that the tight family associated with (4652) Iannini is probably $\lesssim$5 My old. Unfortunately, Nesvorný *et al.*ś method can not be used to determine ages of asteroid families that are much older than $\approx$10 My, because it is difficult to accurately track the orbits of asteroids on $\gtrsim$10-My time scales.

2. Modeling of Family Spreading via Thermal Forces. A recent analysis has shown that the asteroid families are subject to slow spreading and dispersal via Yarkovsky thermal effect (Bottke *et al.* 2001). Therefore, old families' orbital parameters in (a_P, e_P, i_P) space do not reflect the immediate outcomes of cratering events or catastrophic disruptions. Instead, they reveal how the family members evolved in (a_P, e_P, i_P) space over long timescales by dynamical diffusion and chaotic resonances. On the other hand, tight clusters in (a_P, e_P, i_P) space should represent young families that have not yet had an opportunity to disperse via dynamical mechanisms. Using theoretical models of the Yarkovsky effect, Nesvorný *et al.* (2005b) and Vokrouhlický *et al.* (2005a,b) have estimated ages for 25 asteroid families. Vokrouhlický *et al.*ś method is more refined and results in smaller error bars if the assumed albedo values, p_v, are correct. The ages listed in Table 1 for Eos, Agnia, Erigone, Massalia, Merxia and Astrid families assume $p_v = 0.13$, 0.17, 0.05, 0.21, 0.22, 0.08, respectively (Vokrouhlický *et al.* 2005a,b).

https://doi.org/10.1017/S1743921305006800 Published online by Cambridge University Press

The ages were not determined for several families listed in Table 1 due to various reasons. (3) Juno and (4) Vesta families correspond to cratering events for which the contribution of ejection speeds to the present spreads of families in $a_{\rm P}$ is probably very large (Asphaug 1997) making it difficult to separate this contribution from the subsequent spreading by thermal effects. (44) Nysa-Polana clan is a case of two families that overlap in $a_{\rm P}, e_{\rm P}, i_{\rm P}$ space and are difficult to separate (e.g., Cellino *et al.* 2002). (87) Sylvia family is located in a dynamically complicated region at $a_{\rm P} \sim 3.5$ AU where chaotic resonances (rather than thermal effects) determine the dynamical structure of a family. Similarly, (46) Hestia and (2980) Cameron families (both S-type) were affected by strong chaotic resonances in the past (e.g., the 3:1 mean motion resonance for the Hestia family) that removed large fractions of their original populations. The dynamical structures of these families is complex. (18405) FY12 family has only eleven known members. For this reason, its age cannot be reliably determined by methods described above that are statistical in nature. Finally, (137) Meliboea family is a C-type family in the outer main belt that is probably very old because of its large spread in $a_{\rm P}, e_{\rm P}, i_{\rm P}$. A large fraction of dynamical interlopers ($\sim 30\%$ based on the SDSS colors) and the difficulty with choosing an adequate $d_{\rm cutoff}$ prevents us from better estimating the age of this family.

References

Asphaug, E. 1997, *Meteoritics and Planetary Science* 32, 965–980.

Bendjoya, P. & Zappalà, V. 2002, in: W. F. Bottke, A. Cellino, P. Paolicchi & R.P. Binzel (eds.), *Asteroids III*, (Tucson: Univ. Arizona Press), p. 613

Bottke, W.F., Vokrouhlický, D. Brož, M., Nesvorný, D., & Morbidelli, A. 2001 *Science* 294, 1693

Bottke, W.F., Vokrouhlický, D. Rubincam, D.P., & Brož, M. 2002, in: W.F. Bottke, A. Cellino, P. Paolicchi & R. Binzel (eds.), *Asteroids III*, (Tucson: Univ. Arizona Press), p. 395

Bottke, W.F., Durda, D.D., Nesvorný, D., Jedicke, R., Morbidelli, A., Vokrouhlický, D., & Levison, H. 2005, *Icarus* 175, 111

Bowell E., Muinonen, K., & Wasserman, L.H. 1994, in: A. Milani (eds.), *Asteroids, Comets and Meteors*, (Dordrecht: Kluwer), p. 477

Bus, S.J. & Binzel, R.P. 2002a., *Icarus* 158, 106

Bus, S.J. & Binzel, R.P. 2002b., *Icarus* 158, 146

Cellino, A., Zappalà, V., Doressoundiram, A., Di Martino, M., Bendjoya, P., Dotto, E., & Migliorini, F. 2001, *Icarus* 152, 225

Cellino, A., Bus, S.J., Doressoundiram, A., & Lazzaro D. 2002, in: W.F. Bottke, A. Cellino, P. Paolicchi & R.P. Binzel (eds.) *Asteroids III*, (Tucson: Univ. Arizona Press), p. 633

Davis, D.R., Durda, D.D., Marzari, F., Campo Bagatin, A., & Gil-Hutton R. 2002, in: W.F. Bottke, A. Cellino, P. Paolicchi & R.P. Binzel (eds.) *Asteroids III*, (Tucson: Univ. Arizona Press), p. 545

Durda, D.D., Bottke, W.F., Nesvorný, D., Enke, B.L., Asphaug, E., & Richardson, D.C. 2005, *Icarus*, to be submitted.

Fukugita, M., Ichikawa, T., Gunn, J.E., Doi, M., Shimasaku, K., & Schneider, D.P. 1996, *Astron. J.* 111, 1748

Hirayama, K. 1918, *Astron. J.* 31, 185

Ivezić, Ž., and 32 colleagues 2001, *Astron. J.* 122, 2749

Ivezić, Ž., Lupton, R.H., Jurić, M., Tabachnik, S., Quinn, T., Gunn, J.E., Knapp, G.R., Rockosi, C.M., & Brinkmann, J. 2002, *Astron. J.* 124, 2943

Jedicke, R., Nesvorný, D., Whiteley, R., Ivezić, Ž., & Jurić M. 2004, *Nature* 429, 275

Jurić, M., and 15 colleagues 2002, *Astron. J.* 124, 1776

Knežević, Z., Lemaître, A., & Milani, A. 2002, in: W.F. Bottke, A. Cellino, P. Paolicchi & R. Binzel (eds.), *Asteroids III*, (Tucson: Univ. Arizona Press), p. 603

Milani, A. & Knežević, Z. 1994, *Icarus* 107, 219

Morbidelli, A., Nesvorný, D., Bottke, W.F., Michel, P., Vokrouhlický, D., & Tanga, P. 2003, *Icarus* 162, 328

Mothé-Diniz, T., Roig, F., & Carvano, J.M. 2005, *Icarus* 174, 54

Nesvorný, D., Bottke, W.F., Dones, L., & Levison, H.F. 2002a, *Nature* 417, 720

Nesvorný, D., Bottke, W.F., Levison, H.F., & Dones, L. 2003, *Astroph. J.* 591, 486

Nesvorný, D., Enke, B.L., Bottke, W.F., Durda, D.D., Asphaug, E., & Richardson, D.C. 2005a, *Icarus*, submitted.

Nesvorný, D., Jedicke, R., Whiteley, R.J., & Ivezić, Ž. 2005b, *Icarus* 173, 132

Stoughton, C., and 191 colleagues 2002, *Astron. J.* 123, 485

Tanga, P., Cellino, A., Michel, P., Zappalà, V., Paolicchi, P., & dell'Oro, A. 1999, *Icarus* 141, 65

Tedesco, E.F., Noah, P.V., Noah, M., & Price, S.D. 2002, *Astron. J.* 123, 1056

Vokrouhlický, D., Brož, M., Morbidelli, A., Bottke, W.F., Nesvorný, D., Lazzaro, D., & Rivkin, A.S. 2005a, *Icarus*, in press.

Vokrouhlický, D., Brož, M., Bottke, W.F., Nesvorný, D., & Morbidelli, A. 2005b, *Icarus*, in press.

Zappalà, V., Cellino, A., Farinella, P., & Knežević, Z. 1990, *Astron. J.* 100, 2030

Zappalà, V., Cellino, A., Farinella, P., & Milani, A. 1994, *Astron. J.* 107, p. 772

Zappalà, V., Bendjoya, P., Cellino, A., Farinella, P., & Froeschle, C. 1995, *Icarus* 116, 291

Zappalà, V., Cellino, A., Dell'Oro, A., & Paolicchi, P. 2002, in: W.F. Bottke, A. Cellino, P. Paolicchi & R.P. Binzel (eds.), *Asteroids III*, (Tucson: Univ. Arizona Press), p. 619